Structural Basis for Treating Tumor Necrosis Factor α (TNFα)-associated Diseases with the Therapeutic Antibody Infliximab*[S]

Shuaiyi Liang[‡1], Jianxin Dai[§¶1], Sheng Hou[§¶], Lishu Su[‡], Dapeng Zhang[§¶], Huaizu Guo[§¶], Shi Hu[§¶], Hao Wang[§¶], Zihe Rao[‡], Yajun Guo[§¶‖2], and Zhiyong Lou[‡3]

From the ‡Laboratory of Structural Biology and Ministry of Education Laboratory of Protein Science, School of Medicine, Tsinghua University, Beijing 100084, China, §International Joint Cancer Institute, The Second Military Medical University, Shanghai 200433, China, ¶National Engineering Research Center for Antibody Medicine and Shanghai Key Laboratory of Cell Engineering and Antibody, Shanghai 201203, China, and ‖People's Liberation Army (PLA) General Hospital Cancer Center, PLA Postgraduate School of Medicine, 28 Fuxing Road, Beijing 100853, China

Background: Although infliximab has high efficacy in treating TNFα-associated diseases, the epitope on TNFα remains unclear.
Results: The crystal structure of the TNFα in complex with the infliximab Fab is reported at a resolution of 2.6 Å.
Conclusion: TNFα E-F loop plays a crucial role in the interaction.
Significance: The structure may lead to understanding the mechanism of mAb anti-TNFα.

Monoclonal antibody (mAb) drugs have been widely used for treating tumor necrosis factor α (TNFα)-related diseases for over 10 years. Although their action has been hypothesized to depend in part on their ability to bind precursor cell surface TNFα, the precise mechanism and the epitope bound on TNFα remain unclear. In the present work, we report the crystal structure of the infliximab Fab fragment in complex with TNFα at a resolution of 2.6 Å. The key features of the TNFα E-F loop region in this complex distinguish the interaction between infliximab and TNFα from other TNF-receptor structures, revealing the mechanism of TNFα inhibition by overlapping with the TNFα-receptor interface and indicating the crucial role of the E-F loop in the action of this therapeutic antibody. This structure also indicates the formation of an aggregated network for the activation of complement-dependent cytolysis and antibody-dependent cell-mediated cytotoxicity, which result in development of granulomatous infections through TNFα blockage. These results provide the first experimental model for the interaction of TNFα with therapeutic antibodies and offer useful information for antibody optimization by understanding the precise molecular mechanism of TNFα inhibition.

Tumor necrosis factor α (TNFα) is an inflammatory cytokine that plays a central role in acute inflammation and is responsible for a diverse range of signaling events within cells that triggers necrosis or apoptosis (1–4). TNFα is mainly produced in activated macrophages and natural killer cells, whereas lower expression is found in a variety of other cells, including fibroblasts, smooth muscle cells, and tumor cells (5). Human TNFα is translated as a 26-kDa membrane-associated form and is then cleaved in the extracellular domain through the action of matrix metalloproteases to release a mature soluble 17-kDa protein (6). TNFβ (also known as lymphotoxin) is another important TNF member, and its primary sequence shares high sequence and structural similarities with TNFα (7, 8). Both TNFα and TNFβ affect a number of normal and neoplastic cell processes.

The correct functioning of TNF requires effective communication with TNF receptors (TNFRs).[4] Currently, two structurally distinct TNFRs, named TNFR1 and TNFR2, have been identified; both bind with the released soluble form and membrane-associated form of TNFα, respectively (9, 10). The binding of TNFα to TNFR1 has been shown to induce apoptosis and lead to activation of transcription factors involved in cell survival and inflammatory responses as well as to initiate the pathways that lead to caspase activation through the TNFR-associated death domain and FAS-associated death domain proteins (11–13). This physiologic relevance suggests that sequestering TNFα could be used to treat human autoimmune diseases (14), and a number of anti-TNFα agents (drugs and mAbs) have been developed to treat patients with TNFα-associated diseases such as Crohn disease, psoriatic arthritis, rheumatoid arthritis, ankylosing spondylitis, and persistent uveitis (15).

Therapeutic mAbs have high efficacy in treating TNFα-associated diseases. Currently, three versions of therapeutic mAbs,

[4] The abbreviations used are: TNFR, TNF receptor; r.m.s.d., root mean square deviation; CDR, complementarity-determining region.

i.e. etanercept (Enbrel®), infliximab (Remicade®), and adalimumab (Humira®), have been approved by the United States Food and Drug Administration. Among them, infliximab is a chimeric antibody composed of a complement-fixing human IgG1 constant region (75%) and a murine-derived antigen-binding variable region (25%) (16). Infliximab was developed in 1993 and was first approved for treating Crohn disease. Its use has since been extended to the treatment of ankylosing spondylitis, psoriatic arthritis, rheumatoid arthritis, and various inflammatory skin diseases (17). Infliximab is known for its ability to neutralize the biological activity of TNFα by binding to the soluble (free floating in the blood) and transmembrane (located on the outer membranes of T cells and similar immune cells) forms of TNFα with high affinity, preventing it from binding to cellular receptors and inducing the lysis of cells that produce TNFα (18, 19). Infliximab affects the TNFα-mediated signaling pathways of cell proliferation, apoptosis, and cytokine suppression (20). Although the binding avidity or affinity between TNFα and infliximab is reportedly variable because of the different measurement methods used, the high binding avidity/affinity results in the formation of stable TNFα-infliximab complexes (21–23). Interestingly, although TNFα shares high sequence and structural similarities with TNFβ, there is no evidence to show that infliximab can neutralize TNFβ (24), which indicates the high specificity of infliximab in interacting with TNFα.

Although crystallographic studies on TNFα-TNFR2 and TNFβ-TNFR1 complexes in past decades provided the breakthrough for understanding how TNF functions through communicating with receptors (8, 25, 26), the experimental structure of TNFα in complex with the therapeutic antibodies remains exclusive, and the precise mechanism and the epitope on TNFα is still unclear (27). In this work, the crystal structure of TNFα in complex with the infliximab Fab fragment is reported at a resolution of 2.6 Å. The crystal structure of the TNFα-infliximab Fab together with the structures of TNFβ-TNFR1 and TNFα-TNFR2 complexes rationalizes the inhibition of TNFα-receptor interaction by overlap between the mAb- and TNFR-binding sites on the TNFα. Moreover, the distinct features of the E-F loop on TNFα in the TNFα-infliximab Fab complex suggest the molecular basis for the specific binding of infliximab to TNFα but not TNFβ. The structure of the TNFα-infliximab Fab complex also indicates the formation of an aggregated network for the inhibition of membrane-associated TNFα function and, therefore, activation of complement-dependent cytolysis and antibody-dependent cell-mediated cytotoxicity, which result in the reported risk of developing granulomatous infection of TNFα blockages. These results lead to a better understanding of the mechanism of mAbs used for treating TNFα-associated diseases and provide a new focus for the design of future drugs that target TNFα with high efficacy and specificity and with fewer adverse effects.

EXPERIMENTAL PROCEDURES

Protein Expression, Purification, and Characterization—The cDNA sequence-encoding residues Val^{77}–Leu^{233} of human TNFα were cloned into the pET-22b(+) vector (Novagen) and transformed into *Escherichia coli* BL21(DE3) cells (Novagen).

The transformed cells were grown in Luria-Bertani (LB) medium at 37 °C until the OD 600 reached 1.5, and protein expression was induced with 0.5 mM isopropyl 1-thio-β-D-galactopyranoside for 4 h. The bacterial cells were incubated in a lysis buffer (PBS) containing 1 mg/ml lysozyme, 1 mM PMSF, and 1% Triton X-100 for 20 min on ice followed by sonication. The cell lysate was cleared by centrifugation (10,000 × *g*) and filtration (0.45 μm). Solid ammonium sulfate was added to the supernatant to a final concentration of 35%, immediately mixed, and incubated on a roller at 4 °C for 2 h. The solution was then cleared by centrifugation (10,000 × *g*). After discarding the precipitate, solid ammonium sulfate was continuously added to the supernatant to a final concentration of 60%, immediately mixed, and incubated on a roller at 4 °C for 4 h. The precipitated protein was pelleted by centrifugation (10,000 × *g*), and the supernatant was discarded. The precipitate was dissolved in PBS (20 mM phosphate, pH 8.0 and 150 mM NaCl) and separated by gel filtration using Superdex 75 (GE Healthcare). After desalting to 20 mM Tris-HCl, pH 8.0, the target fraction was further purified with a 20-column volume linear NaCl gradient elution from high performance Q-Sepharose (GE Healthcare). The purity was confirmed to be >95% using sodium dodecyl sulfate-polyacrylamide electrophoresis (SDS-PAGE) analysis. The bioactivity was measured in a cytotoxicity assay using the TNF-susceptible murine L-929 cell line in the presence of the metabolic inhibitor actinomycin D (28).

Infliximab (29) was cloned, expressed, and purified following reported procedures. Briefly, the EcoRV and XbaI sites were added to the 5′-end of the heavy chain variable region gene (V_H), and an NheI site was added to the 3′-end. The PCR product was cloned into the pGEM-T vector, and its sequence was confirmed by DNA sequencing. V_H was excised through EcoRV and NheI digestion and then inserted into the EcoRV/NheI sites of the pAH4604 vector containing the human γ-1 constant region gene (C_H). The resultant pAH4604-V_H vector was cleaved with XbaI and BamHI, and then the 3.3-kb fragment containing the chimeric rodent/human antibody heavy chain gene was cloned into the pcDNA3.1(−) vector (Invitrogen), which was digested with the same restriction enzymes, yielding the chimeric heavy chain expression vector pcDNA3.1(−)-$V_H C_H$. The human κ chain constant cDNA (C_L) was obtained as a 0.3-kb PCR product derived from pAG4622. The light chain variable region gene (V_L) of infliximab was fused to the 5′-end of the C_L using the overlapping PCR method. The resultant chimeric light chain gene ($V_L C_L$) with a HindIII site upstream of the start codon and an EcoRI site downstream of the stop codon was cloned into the pGEM-T vector, and its sequence was verified. $V_L C_L$ was excised through HindIII and EcoRI digestion and ligated into the pcDNA3.1 Zeo(+) vector (Invitrogen) cleaved with the same restriction enzymes, yielding the chimeric light chain expression vector pcDNA3.1 Zeo(+)$V_L C_L$. The chimeric light and heavy chain expression vectors were co-transfected into Chinese hamster ovary K1 cells using Lipofectamine 2000 reagent (Invitrogen). Stable transfectants were isolated by limiting dilution in the presence of 600 μg/ml G418 and 300 μg/ml Zeocin. The culture supernates from individual cell clones were analyzed for antibody production using a sandwich enzyme-linked immunosorbent

assay. The assay used goat anti-human IgG Fc (Kirkegaard and Perry Laboratories, Inc., Gaithersburg, MD) as the capture antibodies and goat anti-human κ-horseradish peroxidase (HRP) (Southern Biotechnology Associates, Birmingham, AL) as the detecting antibodies. Purified human IgG1/κ (Sigma) was used as the standard control. The clones that produced the highest amount of recombinant antibodies were selected and grown in serum-free medium. The recombinant antibodies were purified using protein A affinity chromatography from the serum-free culture supernatant. The antibody concentrations were determined by absorbance at 280 nm, and the purity was confirmed using SDS-PAGE analysis. Bioactivity was measured in a cytotoxicity antagonist assay using the TNF-susceptible murine L-929 cell line in the presence of the metabolic inhibitor actinomycin D and TNFα. The Fab fragment of infliximab for crystallographic investigation was obtained through papain digestion of infliximab. The digested protein sample was loaded onto a protein A-Sepharose 4 FF column (GE Healthcare), and the Fab fragment eluted in the flow-through was separated from the Fc fragment and further purified using ion-exchange chromatography using a Q-Sepharose FF column (GE Healthcare). The protein sample was concentrated to ~10 mg/ml and then exchanged to a stock buffer containing 10 mM Tris-HCl, pH 8.0 and 100 mM NaCl.

TNFα and infliximab Fab were mixed at a molar ratio of 1:1 and incubated for 10 h at 4 °C to form the complex before crystallization. The mixed protein was further purified using Superdex 200 gel filtration columns (GE Healthcare) following the procedure suggested by the manufacturer. The fractions were analyzed by SDS-PAGE, and the purity was >95%. The purified protein was then concentrated to 30 mg/ml in 20 mM Tris-HCl, pH 7.4 and 150 mM NaCl for crystallization.

Crystallization—Crystallization of the infliximab Fab/TNFα complex was performed at 290 K using the hanging drop vapor diffusion method. The crystals grew in drops consisting of 1.5 μl of protein and 1.5 μl of reservoir solution against 200 μl of reservoir solution. The initial crystal appeared after 3 days of growth in 1.4 M sodium/potassium phosphate, pH 8.2 with poor diffraction quality after initial screening. Sodium citrate (300 mM) was added to the original solution, and crystals with good diffraction quality were obtained after 5 days of growth. The crystals were soaked in a cryoprotectant solution consisting of the reservoir solution and 25% (v/v) glycol and then flash frozen in liquid nitrogen for x-ray diffraction.

X-ray Data Collection, Processing, and Structure Determination—The initial data set for the TNFα-infliximab Fab complex was collected at the BL17A beamline (Photon Factory, Japan) at a resolution of 3.1 Å. The optimized crystals with good diffraction quality were diffracted to 2.6-Å resolution at 100 K in the Beijing Synchrotron Radiation Facility 3W1A and Shanghai Synchrotron Radiation Facility BL17U beamlines at a wavelength of 1.0000 Å with Mar165 and Mar225 charge-coupled device detectors, respectively. The data were processed, integrated, and scaled using the HKL2000 package (30). The crystals belong to space group *H*3 with cell parameters $a = b = 154.0$ Å, $c = 99.3$ Å, $\alpha = \beta = 90°$, and $\gamma = 120°$. Only one complex molecule per asymmetric unit with a Matthews coefficient of 3.7 Å^3/Da was present, corresponding

to 63.4% solvent content (31). The statistical analysis of all data is presented in Table 1.

The infliximab Fab-TNFα structure was solved by molecular replacement using the crystal structures of apo-TNFα (Protein Data Bank code 1TNF), the light chain of the mAb cetuximab/Erbitux/IMC-C225 (Protein Data Bank code 1YY8), and the heavy chain of humanized antibody C25 Fab fragment (Protein Data Bank code 2GCY) as the initial search models using the program PHASER (32). The structures of uncomplexed light chain from the mAb cetuximab/Erbitux/IMC-C225 and heavy chain from humanized antibody C25 Fab fragment were also used to represent the free form of infliximab Fab. The clear solutions in both the rotation and translation functions indicated the presence of one complex molecule, including one TNFα and one infliximab Fab molecule, in one asymmetric unit, which is consistent with the Matthews coefficient and solvent content (33). Residues that differ between infliximab and the searching model were manually rebuilt in the program Coot (34) under the guidance of the $F_o - F_c$ and $2F_o - F_c$ electron density maps.

After the refinement of the model using simulated annealing, energy minimization, restrained individual B factors, and addition of 83 solvent molecules in PHENIX (35), the respective working R factor and R_{free} dropped from 0.37 and 0.45 to 0.19 and 0.23, respectively, for all data from 50.0 to 2.6 Å. Refinement was monitored by calculating R_{free} based on a subset containing 5% of the total reflections. Model geometry was verified using the program PROCHECK (36). Data collection and refinement statistics are detailed in Table 1. All structure figures were prepared using PyMOL (37).

Competitive Binding Assay—A 96-well plate was coated overnight at 4 °C with 100 μl of recombinant human TNFα (5 μg/ml). Blocking treatment was performed at 37 °C for 2 h. Before addition to the coated plate, different dilutions of infliximab were incubated with 3 μg/ml biotin-labeled Yisaipu® (recombinant human TNFR2-Fc fusion protein, also known as etanercept, which is biosimilar to Enbrel; a product of CPGJ Pharmaceutical, Ltd., Shanghai, China) in PBS. Preincubation mixtures were added to the coated plate. After 2 h of incubation at 37 °C, the wells were washed, and an appropriate dilution of HRP-conjugated avidin was used for detection. After the addition of *tetramethylbenzidine* and stop solution, the absorbance was read at 450 nm with a microplate reader. The percentage of inhibition was calculated using the following formula: Percent inhibition = $(A_{450} \text{ max} - A_{450} \text{ sample})/(A_{450} \text{ max} - A_{450} \text{ blank}) \times 100$.

Kinetics and Binding Assay of TNFα Mutants—E-F loop replacement mutants (into GGGG and SGGSGGSGGSG) and site-directed mutants (Q67A, K112A, R138A, and Y141A) were created using PCR. The mutants were expressed and purified as described for wild-type protein. The infliximab Fab was immobilized onto the surface of a CM-5 sensor chip (GE Healthcare) via amine coupling following the manufacturer's instructions. Maximal electrostatic interaction was obtained with 10 mM sodium acetate, pH 5.0 (data not shown). Infliximab Fab immobilization levels ranging from ~1,000 to 1,500 resonance units were regularly obtained. For binding experiments, the BIAcore T100 (GE Healthcare) instrument was operated at 25 °C, and

the assay buffer was PBS (20 mM phosphate, pH 7.0 and 150 mM NaCl). The contact time (the period during which the analyte, TNFα mutants 4 and 11, was perfused over the chip) was limited to 300 s, and the flow rate was set at 30 μl/min. For chip surface regeneration, a 10 mM glycine, pH 2.0 solution was used to dissociate the bound TNF at the end of each experiment while retaining surface integrity.

Accession Code—The coordinates and structural factors of infliximab Fab in complex with TNFα were deposited in the Protein Data Bank under accession code 4G3Y.

RESULTS

Overall Structure of the TNFα-Infliximab Fab Complex—To elucidate the mechanism of TNFα inhibition through the therapeutic antibody infliximab, the Fab fragment of infliximab and functional TNFα were co-purified and crystallized. The crystal structure of the TNFα-infliximab Fab complex was determined using the molecular replacement method and refined to 2.6-Å resolution with a final R_{work} value of 19.4% (R_{free} = 23.9%) in

TABLE 1
Data collection and refinement statistics

Parameters	Infliximab Fab-TNFα complex
Data collection statistics	
Cell parameters	$a = b = 154.0$ Å, $c = 99.3$ Å, $\alpha = \beta = 90°$, $\gamma = 120°$
Space group	$H3$
Wavelength used (Å)	1.000
Resolution (Å)	50.0 (2.7)^a–2.6
No. of all reflections	156,133
No. of unique reflections	27,025
Completeness (%)	99.0 (94.9)
Average $I/\sigma(I)$	7.6 (2.1)
$R_{merge}{}^b$ (%)	9.2 (47.4)
Refinement statistics	
No. of reflections used ($\sigma(F) > 0$)	25,400
$R_{work}{}^c$ (%)	19.4
$R_{free}{}^c$ (%)	23.9
r.m.s.d. bond distance (Å)	0.009
r.m.s.d. bond angle (°)	1.249
Average overall B value (Å^2)	32.9
Ramachandran plot (excluding Pro and Gly)	
Residues in most favored regions	422 (84.3%)
Residues in additionally allowed regions	80 (15.5%)

^{a} Numbers in parentheses are corresponding values for the highest resolution shell (2.5–2.4 Å).

^{b} $R_{merge} = \Sigma_h\Sigma_i|I_{ih}-I_h|/\Sigma_h\Sigma_i I_h$ where I_h is the mean of multiple observations I_{ih} of a given reflection h.

^{c} $R_{work} = \Sigma\|F_p(\text{obs})|-|F_p(\text{calc})\|/\Sigma|F_p(\text{obs})|$; R_{free} is an R factor for a selected subset (5%) of reflections that was not included in prior refinement calculations.

space group $H3$ (Table 1). Although there is only one TNFα-infliximab Fab complex molecule in one asymmetric unit, the structure revealed a central TNFα trimer bound by three symmetrically arranged infliximab Fab molecules related through a crystallographic 3-fold axis (Fig. 1). This observation is analogous to the structures of TNFα-TNFR2 (26) and TNFβ-TNFR1 (8) complexes and TNFα in complex with other proteins (38), indicating a 3:3 molar ratio for TNFα and infliximab Fab and consistent with the results of the gel filtration and analytical ultracentrifugation (data not shown here).

Only one TNFα molecule is present per asymmetric unit together with one bound infliximab Fab, but three TNFα molecules form a triangular conelike homotrimer associated through a crystallographic 3-fold axis (Fig. 1). Each TNFα molecule contains two packed antiparallel eight-stranded β-sheets, one inner and one outer, in a β-jelly roll topology as well as three additional N-terminal β-strands. The inner sheet, hidden in the trimer complex, is formed by strands B″-B-I-D-G in the correct spatial order, whereas the exposed outer sheet is formed by strands C′-C-H-E-F. Leu-29, Arg-31, Ser-52, and Tyr-56, which are crucial for TNFα cytotoxicity and TNFR binding affinity (2), were confirmed to have the correct conformation by cytotoxicity as described previously (28) (supplemental Fig. S1). Moreover, superimposing the TNFα in the TNFα-infliximab Fab complex with wild-type TNFα yielded a root mean square deviation (r.m.s.d.) of 1.4 Å for the C$^\alpha$ atoms of all residues and indicated no significant overall structural difference between free TNFα and TNFα in complex except for the residues at the antibody-antigen interface.

The E-F loop of TNFα in the TNFα-infliximab Fab complex that plays a crucial role in the antigen-antibody interaction is well ordered and defined by unambiguous electron density (supplemental Fig. S2). However, this region in the TNFα-TNFR2 complex is totally unobservable (26), suggesting a flexible conformation and lack of interaction in the TNFα-TNFR2 complex and indicating a different role of the E-F loop in antibody or receptor binding. Moreover, the E-F loop region in the TNFα-infliximab Fab complex structure displays an extremely large r.m.s.d. value for C$^\alpha$ atoms compared with the free form, indicating that a large conformational change occurs in the loop when TNFα binds with the antibody, whereas a homologous loop region is completely absent in TNFβ (Fig. 2).

FIGURE 1. **Overall structure of the TNFα-infliximab Fab complex.** The TNFα-infliximab Fab complex is shown as a ribbon diagram in two orientations: top view looking down the crystallographic 3-fold symmetry axis (*left*), and side view with the crystallographic 3-fold axis vertical (*right, middle*). The molecules in one TNFα trimer are colored *green*, *light blue*, and *cyan*, respectively. The light chain and heavy chain of infliximab Fab are colored *gold* and *purple*, respectively.

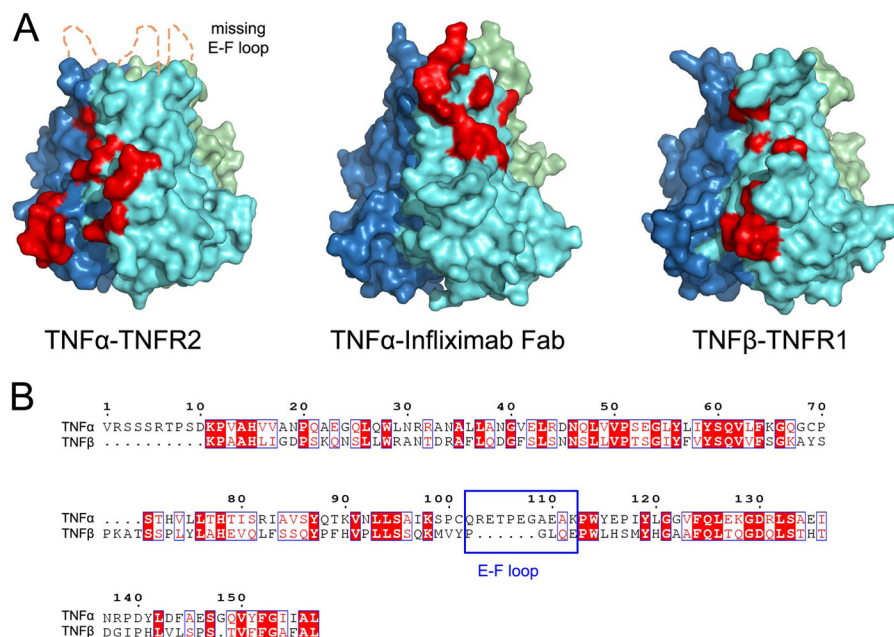FIGURE 2. **Comparison of the interface between TNFα and receptors and infliximab Fab.** *A*, TNFα from the complex structures is represented as a colored surface with TNFR2 and the infliximab Fab interface highlighted in *red* at one of three interfaces on the TNFα trimer. The E-F loop region, which is missing in the TNFα-TNFR2 complex because of the lack of interaction, is labeled. The TNFβ from the TNFβ-TNFR1 complex structure is shown as a colored surface with one of the TNFR1-binding sites highlighted in *red*. All TNF molecules are superposed and presented in the same orientation. *B*, the amino acid sequence alignment of TNFα and TNFβ. The E-F loop, which may play a central role in antibody-antigen interaction, is *framed*. The numbering of residues (*top*) refers to that in TNFα.

The infliximab Fab molecule presents a canonical immunoglobulin fold consisting of four β-barrel domains. The light chain is composed of residues Asp-1 to Cys-214, which fold into the V_L and C_L domains, and the heavy chain residues Glu-1 to Thr-226 fold into the V_H and C_H domains (except for the last six residues in the C terminus of the heavy chain that are missing because of a lack in density, which indicates a disordered and flexible conformation). Ala-51$_L$, which is located at the classical γ-turn in the immunoglobulin family, displays a disallowed stereochemical geometry similar to its counterparts in other reported Fab structures (39). Intramolecular disulfide bonds are found in the expected positions for typical immunoglobulin Fab molecules: two between Cys-23$_L$/Cys-88$_L$ and Cys-134$_L$/Cys-194$_L$ and two between Cys-22$_H$/Cys-98$_H$ and Cys-147$_H$/Cys-203$_H$. The complementarity-determining regions (CDRs) of the infliximab Fab have an ordinary length without unusual residues according to a Kabat sequence database search (40). The elbow angle of the infliximab Fab, defined as the angle subtended by the two pseudo 2-fold axes relating V_H to V_L and C_H to C_L, is 168° in the TNFα-infliximab Fab complex.

Interactions between TNFα and Infliximab—The infliximab Fab interacts with only one TNFα molecule of a TNFα trimer in the complex structure through a large and highly complementary interface (Figs. 2*A* and 3), which is consistent with the high affinity between infliximab and TNFα. The total buried surface area between infliximab Fab and TNFα is 1,977 Å^2 of which TNFα contributes 1,035 Å^2 and the light and heavy chains of infliximab Fab contribute 450 and 600 Å^2, respectively. This is also larger than typical protein-protein interfaces (1,560–1,700 Å^2) (41). The interaction is demonstrated by a high shape complementarity value (42) of 0.72 (compared with the average shape complementarity value of 0.64–0.68 for antibody-antigen complexes). The comparison between the interfaces of

TNFα-infliximab Fab and TNFα-TNFR2 indicated that the interface of TNFα-infliximab Fab overlaps with the TNFR2-binding site, thus allowing infliximab to inhibit TNFα function.

The interface on TNFα is primarily composed of the C-D and E-F loop residues as well as several key residues in strands C and D that interact with Ile[28]–Trp[33] (in CDR H1), Arg[52]–Asn[57] (in CDR H2), and Tyr[102]–Ser[105] (in CDR H3) in the heavy chain of infliximab Fab. The TNFα G-H loop and additional residues in the C-D loop also bind to His[92]–Trp[94] (in CDR L3) and several other residues in the antibody light chain (*e.g.* Ser-32 in CDR L1 and Tyr-50 in CDR L2) (Fig. 3). There are over 30 pairs of interactions, including hydrogen bonds, salt bridges, and van der Waals contacts, that connect the molecules of TNFα and infliximab Fab in their complex; this indicates a strong and stable interaction between these two proteins and may account for their high binding affinity (Table 2).

Several distinct differences were found by superimposing the TNFβ-TNFR1 or TNFα-TNFR2 complex structure onto the TNFα-infliximab Fab complex structure (Fig. 2). First, TNFα residues Glu[67]–His[73] and Thr[105]–Lys[112], which are located in the C-D and E-F loops, mostly contribute to the interaction between TNFα and infliximab Fab. Although the overall folding of TNFα and its binding with infliximab Fab display nearly the same conformation with an r.m.s.d. of 1.43 Å for 157 C^α atoms, the E-F loop moves outward with the C-D loop that moves toward the infliximab Fab molecule to accommodate the V_H and V_L domains of the antibody (Fig. 4). Additionally, the G-H loop displays another slight shift, but it may not be related to the antibody interaction. In contrast, only a few residues in the C-D loop of TNFβ bind to TNFR, and the key E-F loop region of TNFα is shorter in the TNFβ amino acid sequence (Fig. 2*B*), which is consistent with the absence of this loop region in the TNFβ structure. Furthermore, the E-F loop is completely miss-
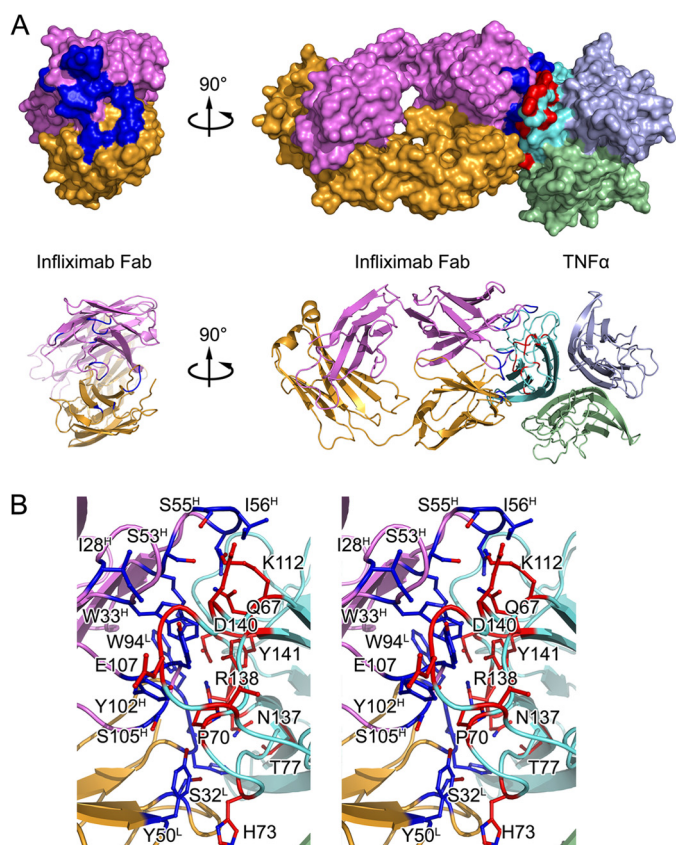
Crystal Structure of TNFα-Infliximab Fab

FIGURE 3. **Detailed TNFα-infliximab Fab interface.** *A*, surface representations and ribbon diagrams of infliximab Fab (*left*) and the TNFα-infliximab Fab complex (*right*). The light chain and heavy chain of infliximab Fab are colored *gold* and *magenta*, respectively. The TNFα trimer is colored *cyan*. The contact surfaces (≤3.6 Å) are highlighted in *blue* on infliximab Fab and *red* on TNFα. Ribbon diagrams corresponding to the surfaces shown above with the same color scheme. *B*, stereoview of the TNFα-infliximab Fab interface. The residues that are involved in the intermolecular interaction are shown as *colored sticks* with the same scheme as the surface representation above. Infliximab Fab and TNFα molecules are presented as *ribbon* diagrams.

TABLE 2

Complete list of interactions between TNFα and infliximab Fab (≤3.6 Å)

TNFα		Infliximab Fab			
Residue	Atom	Residue	Atom	CDR loop	Distance
					Å
Gln-67	C^δ	Ile-56$_H$	$C^{\delta 1}$	H2	3.04
	$O^{\epsilon 1}$	Ile-56$_H$	$C^{\delta 1}$		2.82
	$N^{\epsilon 2}$	Ile-56$_H$	$C^{\delta 1}$		3.18
	$N^{\epsilon 2}$	Ser-53$_H$	O^γ		3.58
	$N^{\epsilon 2}$	Ser-55$_H$	O^γ		3.44
Pro-70	C^β	Ser-105$_H$	O^γ	H3	3.46
	C^β	Tyr-50$_L$	OH	L2	3.45
	C^β	Ser-105$_H$	C^β	H3	3.57
	C^γ	Tyr-103$_H$	O	H3	3.03
Ser-71	C^β	Tyr-50$_L$	$C^{\epsilon 1}$	L2	3.25
	C^β		C^ζ	L2	3.34
His-73	C^β	Tyr-50$_L$	$C^{\delta 2}$	L2	3.50
Thr-105	O	Tyr-102$_H$	OH	H3	2.86
Glu-107	N	Tyr-102$_H$	OH	H3	3.58
	C^α		OH	H3	3.53
	C^β		OH	H3	3.51
Ala-109	O	Tyr-103$_H$	OH	H3	3.22
Glu-110	C^β	Asn-31$_H$	$N^{\delta 2}$	H2	3.53
Asn-137	O	Trp-94$_L$	N	L3	2.92
		Ser-93$_L$	C^α		3.30
		Ser-93$_L$	O^γ		3.55
Asn-137	C^β	Ser-93$_L$	O^γ	L3	3.48
	C^γ	His-92$_L$	O		3.58
	$N^{\delta 2}$	His-92$_L$	O		2.81
	$N^{\delta 2}$	His-92$_L$	$C^{\epsilon 1}$		3.54
	$N^{\delta 2}$	His-92$_L$	$N^{\epsilon 2}$		3.43
Arg-138	C^δ	His-92$_L$	O	L3	3.28
	NH1	Ser-91$_L$	O		3.44
Asp-140	$O^{\delta 1}$	Trp-94$_L$	C^β	L3	3.52
	$O^{\delta 1}$	Trp-94$_L$	C^γ	L3	3.56
	$O^{\delta 2}$	Arg-52$_H$	C^ζ	H2	3.58
	$O^{\delta 2}$	Arg-52$_H$	$N^{\eta 1}$	H2	3.27
	$O^{\delta 2}$	Arg-52$_H$	$N^{\eta 2}$	H2	3.00
Tyr-141	$C^{\epsilon 1}$	Arg-52$_H$	$N^{\eta 1}$	H2	3.43
	OH	Trp-33$_H$	$C^{\eta 2}$	H1	3.35

ing in the TNFα-TNFR2 crystal structure, which indicates that the E-F loop has a flexible conformation and does not participate in the interaction between TNFR2 and TNFα (43). Combined with previous data that indicate that infliximab does not affect the function of TNFβ (24), the TNFα E-F loop may play a central role in the specific interaction between infliximab and TNFα but not TNFβ.

The results of the *in vitro* binding assay revealed that TNFα E-F loop replacement mutants with the residues GGGG (named TNFα(EF-4G)) and SGGSGGSGGSG (named TNFα(EF-11SG)), distinctively increased the K_D value 10^3-fold over the wild-type TNFα (Table 3 and supplemental Fig. S3). This suggests that the E-F loop mutants can decrease the binding affinity and play essential roles in the interaction of TNFα with infliximab Fab. Nonetheless, the TNFα(Q67A) and TNFα(K112A) mutants, which are located in the C-D and E-F loops, respectively, only slightly decreased the binding affinity with infliximab Fab. This indicates that the C-D and E-F loops contribute to the interaction with the antibody through a molecular network but not via individual residues.

The G-H loop residues Asn[137]–Tyr[141] together with Thr-77 in strand D of TNFα interact with the infliximab Fab, consistent with the TNFβ-TNFR1 interaction (8). Arg-138 provides two ideal hydrogen bonds with Ser-91$_L$ and His-92$_L$ from the light chain and, thus, contributes to the interaction between TNFα and the antibody. Tyr-141, which extends its side chain toward the heavy chain of infliximab Fab, provides a large hydrophobic interface (via its side chain) as well as hydrogen bonding with Trp-33$_H$ and Arg-52$_H$ to stabilize the TNFα-infliximab Fab complex.

In concordance with the crystallographic analysis, the results of the *in vitro* binding assays demonstrate that TNFα(R138A) and TNFα(Y141A) mutations significantly decrease the binding of TNFα to infliximab (Table 3). In sharp contrast, the region between A and A′, which participates in TNFβ-TFNR1 binding, is not involved in the TNFα-infliximab Fab interaction. Moreover, TNFα residues Arg-31, Arg-32, and Tyr-87, which are crucial for binding both TNFRs (26, 44), are not involved in the TNFα-infliximab Fab interface, indicating the different binding behavior of TNFα with receptors and antibodies. Furthermore, the groove between two adjacent TNFα subunits is crucial for the interaction between TNFs and TNFRs (8, 26, 38). However, similar structural features are not found in the TNFα-infliximab Fab complex structure. These data indicate that the interaction between TNFs and their receptors or antibodies are likely more complicated than previously suggested based on the structural analysis of TNFα with its receptors (8).

Molecular Mechanism of TNFα Inhibition by Infliximab—Although the molecular coordinates of TNFα and TNFβ that are bound with TNFRs provide an understanding of the mechanism of TNF function, the lack of structural information on TNFα bound to therapeutic antibodies hinders the elucidation of the precise epitope and clear inhibition mechanism of infliximab despite the fact that infliximab therapy has been used for TNFα-associated diseases for over 10 years. In the TNFα-TNFR2 and TNFβ-TNFR1 structures, the cytokine-receptor interface can be conventionally characterized into upper and lower regions, which primarily focus on the D-E and A-A″
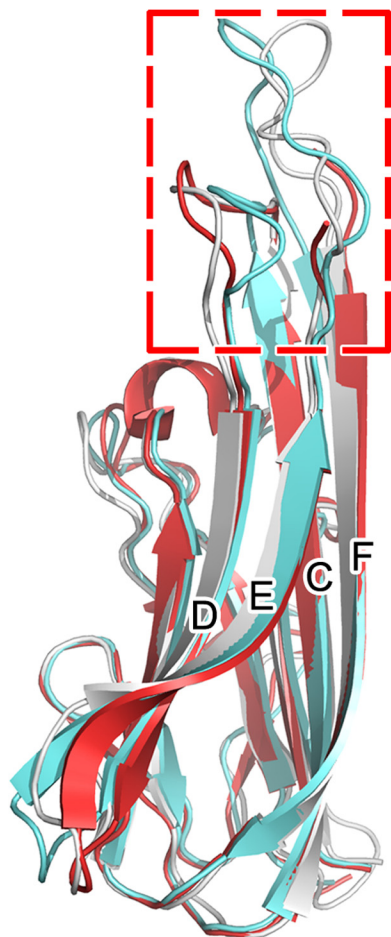

FIGURE 4. **Structural variety of TNFα in free form and TNFα-TNFR2 and TNFα-infliximab Fab complexes.** The free state of the molecule is colored *gray*. TNFα molecules in the TNFα-TNFR2 and TNFα-infliximab Fab complex structures are colored *red* and *cyan*, respectively. The variant parts of the C-D and E-F loops of TNFα are *framed*.

regions, respectively. In the TNFα-infliximab Fab structure, residues Gln[67]–His[73] and Gln[102]–Lys[112] in the TNFα C-D and E-F loops are largely responsible for the antibody-antigen interaction, whereas Asn[137]–Tyr[141] in the G-H loop and Thr-77 in strand D of TNFα complementarily contribute to this interaction.

The solvent-accessible surface contributed by these interactions covers over 60% of the total interface between TNFα and TNFR1, which indicates an overlap between the TNFα receptor-binding sites and the infliximab epitope. Moreover, although several other residues crucial for TNFα-receptor binding do not participate in the TNFα-infliximab Fab interface (especially the groove between two associated TNFα molecules in the TNFα trimer), the peak region of the cone of the TNFα trimer appears to largely contribute to the interaction with infliximab Fab.

These results may explain in part the biochemical data concerning the binding avidity or affinity of infliximab to soluble or membrane-associated TNFα (affinity for soluble TNFα is 27 pM, and avidity for membrane-associated TNFα is 0.45 nM) (23) compared with the binding avidity of TNFR1 to TNFα (0.38 nM) (43). Therefore, the binding of infliximab to TNFα efficiently competes with TNFRs binding to TNFα, and the interface between TNFα and TNFRs is blocked with sufficient amounts of infliximab, thereby preventing TNFα to function further in diseases. Nonetheless, the exact TNFα-receptor interface has still not been elucidated according to current structural investigations (8, 45–47). However, our data suggest that infliximab blocks the TNFα-TNFR interaction by occupying part if not the same TNFα binding interface.

DISCUSSION

TNFα is an inflammatory cytokine that is predominantly produced by activated macrophages and lymphocytes, plays a central role in acute inflammation, and is responsible for a diverse range of signaling events within cells that lead to necrosis or apoptosis (1, 2). Therefore, the inhibition of TNFα is a validated and favorable method for treating several important TNFα-associated diseases. Currently, several receptors are known to interact with TNFα and, thus, play a key role in TNFα-associated diseases. Therefore, an extensive range of TNFα-inhibitory proteins, most of which are based on an antibody scaffold, have been developed and used with variable success as therapeutic agents to block the interaction between TNFα and its receptors (48).

TABLE 3

Kinetics and binding of TNFα mutants with infliximab Fab

Kinetics and binding of TNFα mutant and infliximab Fab were analyzed using a BIAcore T100. Wild-type TNFα and the mutants were passed over the immobilized infliximab Fab surface, and the data were globally analyzed using a simultaneous fit for both dissociation (k_d) and association (k_a). The value for K_D was calculated as k_d/k_a. Typical error levels for the k_d and k_a values are less than ±15%.

	k_a	k_d	K_D
	$M^{-1}\cdot s^{-1}$	s^{-1}	M
WT TNFα	$3.50 \pm 0.52 \times 10^4$	$3.0 \pm 0.45 \times 10^{-4}$	$8.70 \pm 1.3 \times 10^{-9}$
TNFα(EF-4G)	$0.96 \pm 0.14 \times 10^4$	$1.7 \pm 0.25 \times 10^{-2}$	$1.78 \pm 0.27 \times 10^{-6}$
TNFα(EF-11SG)	$3.00 \pm 0.45 \times 10^4$	$5.0 \pm 0.75 \times 10^{-2}$	$1.80 \pm 0.27 \times 10^{-6}$
TNFα(Q67A)	$5.86 \pm 0.88 \times 10^3$	$1.80 \pm 0.27 \times 10^{-4}$	$3.07 \pm 0.46 \times 10^{-8}$
TNFα(K112A)	$1.67 \pm 0.25 \times 10^4$	$4.74 \pm 0.71 \times 10^{-4}$	$2.84 \pm 0.43 \times 10^{-8}$
TNFα(R138A)	$1.76 \pm 0.26 \times 10^2$	$1.69 \pm 0.25 \times 10^{-3}$	$9.61 \pm 1.44 \times 10^{-6}$
TNFα(Y141A)	$2.02 \pm 0.30 \times 10^2$	$1.07 \pm 0.16 \times 10^{-3}$	$5.32 \pm 0.80 \times 10^{-6}$

Crystal Structure of TNFα-Infliximab Fab

Infliximab is a therapeutic mAb that was approved by the United States Food and Drug Administration to treat Crohn disease, ankylosing spondylitis, psoriatic arthritis, rheumatoid arthritis, and ulcerative colitis. However, because infliximab is a chimeric mAb and its use is not very well tolerated in the majority of patients, infliximab therapy leads to the production of antibodies to infliximab in a small subset of patients (49–52). Increasing the human sequence content by grafting murine CDRs may be crucial for the integral capacity of antigen binding and should be retained during humanization (53). Therefore, structural evidence concerning the TNFα-infliximab Fab interface could provide direct information for anti-TNFα antibody humanization. Together with infliximab, adalimumab is another widely used (and the first fully human) therapeutic mAb for treating TNFα-associated diseases; it was approved by the United States Food and Drug Administration in 2008 (54). Although adalimumab has a mechanism similar to that of infliximab for treating Crohn disease, rheumatoid arthritis, psoriatic arthritis, and ankylosing spondylitis, the different binding avidities of infliximab (4.2 pM) and adalimumab (8.5 pM) for TNFα (23) suggest variable antigen-antibody interfaces.

Given that the binding affinity between an antibody and an antigen is one of the most important determinants for therapeutic antibody development, improving the surface complementarity of the interface between the antibody and the antigen, strengthening the interaction, and, thus, enhancing the binding affinity through mutagenesis of the paratope of the antibody are of particular interest. Although the interface between infliximab Fab and TNFα has high complementarity with an shape complementarity value of 0.72, the complex structure reported here still provides valuable information for enhancing their binding affinity.

First, the side chain of Gln-67 in the C-D loop of TNFα interacts with the acid cavity formed by the side chains of Ser-53$_H$ and Ser-55$_H$ with relatively long distances (>3.4 Å). Therefore, the substitution of Ser-53$_H$ and Ser-55$_H$ with long side chain acidic residues (*e.g.* aspartate) may provide more favorable interactions with Gln-67$_{TNF}$. Second, the side chain of Trp-94$_L$ provides one van der Waals contact with TNFα residues, mostly with highly charged side chains (*e.g.* aspartate and arginine), which suggests that the substitution of Trp-94$_L$ with a long side chain charged residue may result in more and better interactions with TNFα. Several other substitutions, for example S91$_L$D, S93$_L$D, and N31$_H$Q, could potentially increase the interaction (and thus increase the binding) between infliximab and TNFα. Nonetheless, the complexity of antibody-antigen interaction requires further testing and validation. Moreover, because the E-F loop is the most divergent portion between TNFα and TNFβ (in both amino acid sequence and three-dimensional structure) and may play a central role in the specific interaction between TNFα and infliximab, improving the E-F loop-interacting region is crucial for increasing the mAb binding and avoiding the side effects caused by interacting with TNFβ in host cells. Notably, although E-F is essential for the binding of infliximab to TNFα, there is no evidence to show that this fragment is important to the biological function of TNFα. The structure of TNFα-TNFR2 also revealed that E-F loop does not participate in the binding to TNFRs (26). There-fore, the binding of infliximab to the TNFα E-F loop is not likely to directly impact the function of TNFα but only spatially affect the communication between TNFα and TNFRs.

REFERENCES

1. Carter, P. H., Scherle, P. A., Muckelbauer, J. K., Voss, M. E., Liu, R. Q., Thompson, L. A., Tebben, A. J., Solomon, K. A., Lo, Y. C., Li, Z., Strzemienski, P., Yang, G., Falahatpisheh, N., Xu, M., Wu, Z., Farrow, N. A., Ramnarayan, K., Wang, J., Rideout, D., Yalamoori, V., Domaille, P., Underwood, D. J., Trzaskos, J. M., Friedman, S. M., Newton, R. C., and Decicco, C. P. (2001) Photochemically enhanced binding of small molecules to the tumor necrosis factor receptor-1 inhibits the binding of TNF-α. *Proc. Natl. Acad. Sci. U.S.A.* **98,** 11879–11884
2. Idriss, H. T., and Naismith, J. H. (2000) TNFα and the TNF receptor superfamily: structure-function relationship(s). *Microsc. Res. Tech.* **50,** 184–195
3. An, Z. (2010) Monoclonal antibodies—a proven and rapidly expanding therapeutic modality for human diseases. *Protein Cell* **1,** 319–330
4. Ono, K., Wang, X., Kim, S. O., Armstrong, L. C., Bornstein, P., and Han, J. (2010) Metaxin deficiency alters mitochondrial membrane permeability and leads to resistance to TNF-induced cell killing. *Protein Cell* **1,** 161–173
5. van Horssen, R., Ten Hagen, T. L., and Eggermont, A. M. (2006) TNF-α in cancer treatment: molecular insights, antitumor effects, and clinical utility. *Oncologist* **11,** 397–408
6. Chiou, H. L., Lee, T. S., Kuo, J., Mau, Y. C., and Ho, M. S. (1997) Altered antigenicity of 'a' determinant variants of hepatitis B virus. *J. Gen. Virol.* **78,** 2639–2645
7. Perez, C., Albert, I., DeFay, K., Zachariades, N., Gooding, L., and Kriegler, M. (1990) A nonsecretable cell surface mutant of tumor necrosis factor (TNF) kills by cell-to-cell contact. *Cell* **63,** 251–258
8. Banner, D. W., D'Arcy, A., Janes, W., Gentz, R., Schoenfeld, H. J., Broger, C., Loetscher, H., and Lesslauer, W. (1993) Crystal structure of the soluble human 55 kd TNF receptor-human TNFβ complex: implications for TNF receptor activation. *Cell* **73,** 431–445
9. Chan, K. F., Siegel, M. R., and Lenardo, J. M. (2000) Signaling by the TNF receptor superfamily and T cell homeostasis. *Immunity* **13,** 419–422
10. Palladino, M. A., Bahjat, F. R., Theodorakis, E. A., and Moldawer, L. L. (2003) Anti-TNF-α therapies: the next generation. *Nat. Rev. Drug Discov.* **2,** 736–746
11. Aggarwal, B. B. (2003) Signalling pathways of the TNF superfamily: a double-edged sword. *Nat. Rev. Immunol.* **3,** 745–756
12. Pfeffer, K., Matsuyama, T., Kündig, T. M., Wakeham, A., Kishihara, K., Shahinian, A., Wiegmann, K., Ohashi, P. S., Krönke, M., and Mak, T. W. (1993) Mice deficient for the 55 kd tumor necrosis factor receptor are resistant to endotoxic shock, yet succumb to *L. monocytogenes* infection. *Cell* **73,** 457–467
13. Chen, G., and Goeddel, D. V. (2002) TNF-R1 signaling: a beautiful pathway. *Science* **296,** 1634–1635
14. Moreland, L. W. (1999) Inhibitors of tumor necrosis factor for rheumatoid arthritis. *J. Rheumatol. Suppl.* **57,** 7–15
15. Hasegawa, A., Takasaki, W., Greene, M. I., and Murali, R. (2001) Modifying TNFα for therapeutic use: a perspective on the TNF receptor system. *Mini Rev. Med. Chem.* **1,** 5–16
16. Knight, D. M., Trinh, H., Le, J., Siegel, S., Shealy, D., McDonough, M., Scallon, B., Moore, M. A., Vilcek, J., Daddona, P., and Ghrayeb, J. (1993) Construction and initial characterization of a mouse-human chimeric anti-TNF antibody. *Mol. Immunol.* **30,** 1443–1453
17. Gupta, A. K., and Skinner, A. R. (2004) A review of the use of infliximab to manage cutaneous dermatoses. *J. Cutan. Med. Surg.* **8,** 77–89
18. Ricart, E., and Sandborn, W. J. (1999) Infliximab for the treatment of fistulas in patients with Crohn's disease. *Gastroenterology* **117,** 1247–1248
19. Talbot, C., Sagar, P. M., Johnston, M. J., Finan, P. J., and Burke, D. (2005)

Infliximab in the surgical management of complex fistulating anal Crohn's disease. *Colorectal Dis.* **7,** 164–168

20. Tracey, D., Klareskog, L., Sasso, E. H., Salfeld, J. G., and Tak, P. P. (2008) Tumor necrosis factor antagonist mechanisms of action: a comprehensive review. *Pharmacol. Ther.* **117,** 244–279

21. Scallon, B., Cai, A., Solowski, N., Rosenberg, A., Song, X. Y., Shealy, D., and Wagner, C. (2002) Binding and functional comparisons of two types of tumor necrosis factor antagonists. *J. Pharmacol. Exp. Ther.* **301,** 418–426

22. Scallon, B. J., Moore, M. A., Trinh, H., Knight, D. M., and Ghrayeb, J. (1995) Chimeric anti-TNF-α monoclonal antibody cA2 binds recombinant transmembrane TNF-α and activates immune effector functions. *Cytokine* **7,** 251–259

23. Kaymakcalan, Z., Sakorafas, P., Bose, S., Scesney, S., Xiong, L., Hanzatian, D. K., Salfeld, J., and Sasso, E. H. (2009) Comparisons of affinities, avidities, and complement activation of adalimumab, infliximab, and etanercept in binding to soluble and membrane tumor necrosis factor. *Clin. Immunol.* **131,** 308–316

24. Buch, M. H., Conaghan, P. G., Quinn, M. A., Bingham, S. J., Veale, D., and Emery, P. (2004) True infliximab resistance in rheumatoid arthritis: a role for lymphotoxin α? *Ann. Rheum. Dis.* **63,** 1344–1346

25. Jones, E. Y., Stuart, D. I., and Walker, N. P. (1989) Structure of tumour necrosis factor. *Nature* **338,** 225–228

26. Mukai, Y., Nakamura, T., Yoshikawa, M., Yoshioka, Y., Tsunoda, S., Nakagawa, S., Yamagata, Y., and Tsutsumi, Y. (2010) Solution of the structure of the TNF-TNFR2 complex. *Sci. Signal.* **3,** ra83

27. Kim, M. S., Lee, S. H., Song, M. Y., Yoo, T. H., Lee, B. K., and Kim, Y. S. (2007) Comparative analyses of complex formation and binding sites between human tumor necrosis factor-α and its three antagonists elucidate their different neutralizing mechanisms. *J. Mol. Biol.* **374,** 1374–1388

28. Matthews, N., and Neale, M. L. (1987) *Lymphokines and Interferons, a Practical Approach*, IRL Press, Oxford

29. Le, J. M., Vilcek, J., Dadonna, P., Ghrayeb, J., Knight, D., and Siegel, S. A. (August 12, 1997) U. S. Patent 5,656,272

30. Otwinowski, Z., and Minor, W. (1997) in *Macromolecular Crystallography, Part A* (Carter Jr., C. W., and Sweet, R. M., eds) pp. 307–326, Academic Press, New York

31. *Collaborative Computational Project, Number 4* (1994) The CCP4 suite: programs for protein crystallography. *Acta Crystallogr. D Biol. Crystallogr.* **50,** 760–763

32. McCoy, A. J., Grosse-Kunstleve, R. W., Storoni, L. C., and Read, R. J. (2005) Likelihood-enhanced fast translation functions. *Acta Crystallogr. D Biol. Crystallogr.* **61,** 458–464

33. Matthews, B. W. (1968) Solvent content of protein crystals. *J. Mol. Biol.* **33,** 491–497

34. Emsley, P., and Cowtan, K. (2004) Coot: model-building tools for molecular graphics. *Acta Crystallogr. D Biol. Crystallogr.* **60,** 2126–2132

35. Adams, P. D., Grosse-Kunstleve, R. W., Hung, L. W., Ioerger, T. R., McCoy, A. J., Moriarty, N. W., Read, R. J., Sacchettini, J. C., Sauter, N. K., and Terwilliger, T. C. (2002) PHENIX: building new software for automated crystallographic structure determination. *Acta Crystallogr. D Biol. Crystallogr.* **58,** 1948–1954

36. Laskowski, R., MacArthur, M., Moss, D., and Thornton, J. (1993) PROCHECK: a program to check the stereochemical quality of protein structures. *J. Appl. Crystallogr.* **26,** 283–291

37. DeLano, W. L. (2002) *The PyMOL Molecular Graphics System*, Schrödinger, LLC, New York

38. Yang, Z., West, A. P., Jr., and Bjorkman, P. J. (2009) Crystal structure of TNFα complexed with a poxvirus MHC-related TNF binding protein. *Nat. Struct. Mol. Biol.* **16,** 1189–1191

39. Al-Lazikani, B., Lesk, A. M., and Chothia, C. (1997) Standard conformations for the canonical structures of immunoglobulins. *J. Mol. Biol.* **273,** 927–948

40. Martin, A. C. (1996) Accessing the Kabat antibody sequence database by computer. *Proteins* **25,** 130–133

41. Jones, S., and Thornton, J. M. (1996) Principles of protein-protein interactions. *Proc. Natl. Acad. Sci. U.S.A.* **93,** 13–20

42. Lawrence, M. C., and Colman, P. M. (1993) Shape complementarity at protein/protein interfaces. *J. Mol. Biol.* **234,** 946–950

43. Murali, R., Cheng, X., Berezov, A., Du, X., Schön, A., Freire, E., Xu, X., Chen, Y. H., and Greene, M. I. (2005) Disabling TNF receptor signaling by induced conformational perturbation of tryptophan-107. *Proc. Natl. Acad. Sci. U.S.A.* **102,** 10970–10975

44. Mukai, Y., Shibata, H., Nakamura, T., Yoshioka, Y., Abe, Y., Nomura, T., Taniai, M., Ohta, T., Ikemizu, S., Nakagawa, S., Tsunoda, S., Kamada, H., Yamagata, Y., and Tsutsumi, Y. (2009) Structure-function relationship of tumor necrosis factor (TNF) and its receptor interaction based on 3D structural analysis of a fully active TNFR1-selective TNF mutant. *J. Mol. Biol.* **385,** 1221–1229

45. Eck, M. J., and Sprang, S. R. (1989) The structure of tumor necrosis factor-α at 2.6 Å resolution. Implications for receptor binding. *J. Biol. Chem.* **264,** 17595–17605

46. Eck, M. J., Ultsch, M., Rinderknecht, E., de Vos, A. M., and Sprang, S. R. (1992) The structure of human lymphotoxin (tumor necrosis factor-β) at 1.9-Å resolution. *J. Biol. Chem.* **267,** 2119–2122

47. Naismith, J. H., Devine, T. Q., Brandhuber, B. J., and Sprang, S. R. (1995) Crystallographic evidence for dimerization of unliganded tumor necrosis factor receptor. *J. Biol. Chem.* **270,** 13303–13307

48. Byla, P., Andersen, M. H., Holtet, T. L., Jacobsen, H., Munch, M., Gad, H. H., Thøgersen, H. C., and Hartmann, R. (2010) Selection of a novel and highly specific tumor necrosis factor α (TNFα) antagonist: insight from the crystal structure of the antagonist-TNFα complex. *J. Biol. Chem.* **285,** 12096–12100

49. Bachmann, F., Nast, A., Sterry, W., and Philipp, S. (2010) Safety and efficacy of the tumor necrosis factor antagonists. *Semin. Cutan. Med. Surg.* **29,** 35–47

50. Alonso-Ruiz, A., Pijoan, J. I., Ansuategui, E., Urkaregi, A., Calabozo, M., and Quintana, A. (2008) Tumor necrosis factor α drugs in rheumatoid arthritis: systematic review and metaanalysis of efficacy and safety. *BMC Musculoskelet. Disord.* **9,** 52

51. Wiens, A., Venson, R., Correr, C. J., Otuki, M. F., and Pontarolo, R. (2010) Meta-analysis of the efficacy and safety of adalimumab, etanercept, and infliximab for the treatment of rheumatoid arthritis. *Pharmacotherapy* **30,** 339–353

52. Baidoo, L., and Lichtenstein, G. R. (2005) What next after infliximab? *Am. J. Gastroenterol.* **100,** 80–83

53. Bernett, M. J., Karki, S., Moore, G. L., Leung, I. W., Chen, H., Pong, E., Nguyen, D. H., Jacinto, J., Zalevsky, J., Muchhal, U. S., Desjarlais, J. R., and Lazar, G. A. (2010) Engineering fully human monoclonal antibodies from murine variable regions. *J. Mol. Biol.* **396,** 1474–1490

54. Mazza, J., Rossi, A., and Weinberg, J. M. (2010) Innovative uses of tumor necrosis factor α inhibitors. *Dermatol. Clin.* **28,** 559–575